

# Effect of sputtering time processes on phase transformation, optical and photoelectrical properties of CuInSe<sub>2</sub> film solar cells

XIN JI<sup>\*</sup>, LIN JUN WANG, JIAN YONG TENG, YI MING MI<sup>a</sup>, CHAO MIN ZHANG<sup>a</sup>

*School of Materials Science & Engineering, Shanghai University, Shanghai 200444, China*

*<sup>a</sup>College of Fundamental Studies, Shanghai University of Engineering Science, Shanghai 201620, China*

Sputtering deposited CuInSe<sub>2</sub> films are of potential important as absorber material in thin-film solar cells as long as we can optimize the sputtering time processes to enhance their photoelectrical properties. The results show that long-time sputtering processes exceeding to 3.0h can produce the particle aggregation and clusters to enhance the conversion efficiency of CuInSe<sub>2</sub> solar cells. Long-time sputtering processes (2.5, 3.0 and 4.0h) are found to be vital for the transformation from the InxSe phase to In<sub>2</sub>Se<sub>3</sub> and InSe structures. In addition, the optical absorbance result show that the optical absorbance of CIS film at 4.0 h is higher than the other films in the wavelength region above 300 nm. Also, the long-time sputtering processes (3.0 and 4.0h) can cause a significant increase in the optical band gap close to the best absorbed band gap of sunlight. Finally, the I-V characteristic curves show that the photoelectric conversion efficiency of CIS film batteries increase from 1.14% to 5.56% and short circuit current density increase from 12.63 to 22.26mA/cm<sup>2</sup> with the sputtering time increase from 1.0 to 4.0h.

(Received September 28, 2015; accepted October 28, 2015)

*Keywords:* CuInSe<sub>2</sub> film, Sputtering times, Vapor deposition, Phase transitions, Optical properties, Photoelectrical properties

## 1. Introduction

CuInSe<sub>2</sub> thin films have exceptional material characteristics including band-gap, absorption coefficient and minority carrier diffusion length [1-2]. This combination of properties along with low raw materials cost has made CuInSe<sub>2</sub> a potential candidate for photovoltaic applications [3-4]. CuInSe<sub>2</sub> films can be synthesized by different methods such as RF-magnetron sputtering [5], flash evaporation [6] chemical spray [7] and electro-deposition [8]. Among these techniques the magnetron sputtering has been proved as successful way to improve properties of CuInSe<sub>2</sub> films such as electrical, optical and the photoelectrical properties [9-10]. Also, the material transfer by sputtering process during magnetron deposition provides the means to synthesize photoelectrical compound films [11-12]. Additionally, magnetron sputtering has the advantage of producing a nano-crystal structure during the synthesis of photoelectrical compound films [13-14].

Many research efforts have been attempted to develop the sputtering parameters with the ability to form the CuInSe<sub>2</sub> films of better photoelectrical properties [15-16]. Also, there is a growing interest in improving the photoelectrical properties of the CuInSe<sub>2</sub> films, but few satisfactory results have been obtained [17-18]. Although the photoelectrical properties of the CuInSe<sub>2</sub> films are

strongly dependent on the sputtering times in processes, presently there are no references on the systematic research on it [19].

In this work, the transition of crystalline phase and improvement of the photoelectrical properties of CuInSe<sub>2</sub> films at various sputtering times were studied, the objective of this work is to find way of enhance the structural and photoelectrical properties of CuInSe<sub>2</sub> films occurring in the sputtering time processes. The related results and discussions would be feasible for the potential applications of CuInSe<sub>2</sub> films.

## 2. Experiment

### 2.1 Synthesis of CIS thin films

Solar cells were fabricated with the structure SFO/CdS/CIS. A CdS buffer layer was deposited first on an SFO (SnO<sub>2</sub>: F) glass using 50 W power, and then the CIS adsorbed layer was deposited at 100 W power on the CdS window layer. Thin films of CIS and CdS were all deposited by radiofrequency sputtering using a magnetron sputtering system (FJL560D2). Cylindrical CuInSe<sub>2</sub> (Cu:In:Se = 1:1:2) and CdS ceramic targets of 8 cm in diameter were used. No changes in target composition were observed with time and usage. The deposition

chamber's base pressure was  $1.6 \times 10^{-4}$  Pa, and during deposition, the gas pressures were maintained constant at 0.5 Pa. The substrate-to-target distance was 100 mm. Depositions of CdS layers were performed at room temperature for 25 min, respectively. Finally, the layers of CIS layers were deposited at substrate temperatures (200°C) for different sputtering times (1h, 2h, 2.5h, 3h and 4h).

## 2.2 Characterizations of CIS films

To investigate the crystallographic properties of the films, coupled  $\theta$ - $2\theta$  X-ray diffraction (XRD) scans were performed in the range  $2\theta = 20$ – $80^\circ$  by use of the Cu K $\alpha_1$  line of an X-ray source (Rigaku D/max2550). The surface morphologies of films were examined by scanning electron microscopy (SEM-3400-N). Optical properties of the CIS layers were measured at normal incidence using a double beam ultraviolet visible near infrared spectrophotometer (Shimadzu) with optical transmittance in the photon energy range of  $(1.76$ – $10.56) \times 10^{-19}$  J. Current-voltage (I-V) measurements were performed on a constant light source solar simulator at standard test conditions (25°C, AM1.5).

## 3. Results and discussion

### 3.1 Effects of sputtering time processes on phase transformation

Fig. 1 shows the XRD patterns of the CuInSe<sub>2</sub> films deposited at different sputtering times ranging from 1.0 h, 2.0h, 2.5 h, 3.0h to 4.0 h. All the CuInSe<sub>2</sub> thin films show the characteristic peaks of both chalcopyrite and tetragonal structures. It has been observed that crystallinity of films decrease with increase of sputtering times. The CuInSe<sub>2</sub> thin film prepared with 1.0h shows the highest peak-intensity and maximum number of chalcopyrite and tetragonal characteristic peaks, including CIS (112), CIS (211), CIS (310) and CIS (400), which are included in the other samples. It has also been observed that the full width half maximum (FWHM) steadily decreases with more sputtering times, which indicates that the crystallite size of the particles increase in the film at the longer time. Moreover, it is found that the intensity of CIS (112) and (211) peaks decreases markedly relative to that of CIS (310 and (400) peaks when deposition time increased to higher values of 3.0 and 4.0 h. It is suggested that the long

deposition time will suppress the formation of defect and vacancy on these films.

Meanwhile, In<sub>x</sub>Se, In<sub>2</sub>Se<sub>3</sub> and InSe diffraction peaks appear on the position ( $2\theta=61.5^\circ$ ) as the increase of the sputtering times. It is clearly that the phase transformation from In<sub>x</sub>Se phase to In<sub>2</sub>Se<sub>3</sub> and InSe structures is associated with the evaporation of indium in the sputtering time processes. Evaporation of In happens at the sputtering temperature(200°C) within the shorter time of 1.0 and 2.0 h, which lead the formation of In<sub>x</sub>Se by the reaction with In and Se vapor. With the prolong of the reaction time of In and Se vapor, the In<sub>x</sub>Se phase is dissolved and the In<sub>2</sub>Se<sub>3</sub> and InSe structures are formed.

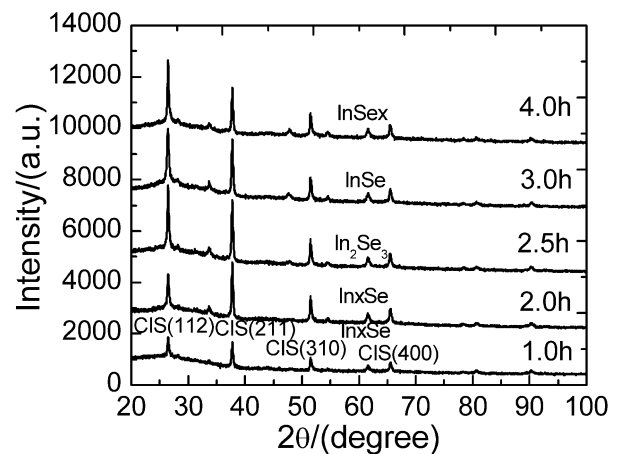


Fig. 1. XRD patterns of CuInSe<sub>2</sub> films prepared at various sputtering times

### 3.2 Effects of sputtering time processes on grain growth

Fig. 2(a)-(e) shows the scanning electron microscopy surface morphologies of CIS films deposited at various sputtering times of 1, 2, 2.5, 3 and 4h, respectively. The surface SEM micrographs of the films are shown in Fig. 3. As shown in Figs. 2(a) and (b), the films deposited at shorter times (1.0 and 2.0 h) have a leaf-shaped particles which the small and black CIS particles scattered around the big white CdS particles. However, the CIS particles of 2.5h (Fig. 3 (c)) show a well grown grain and clear grain boundary.

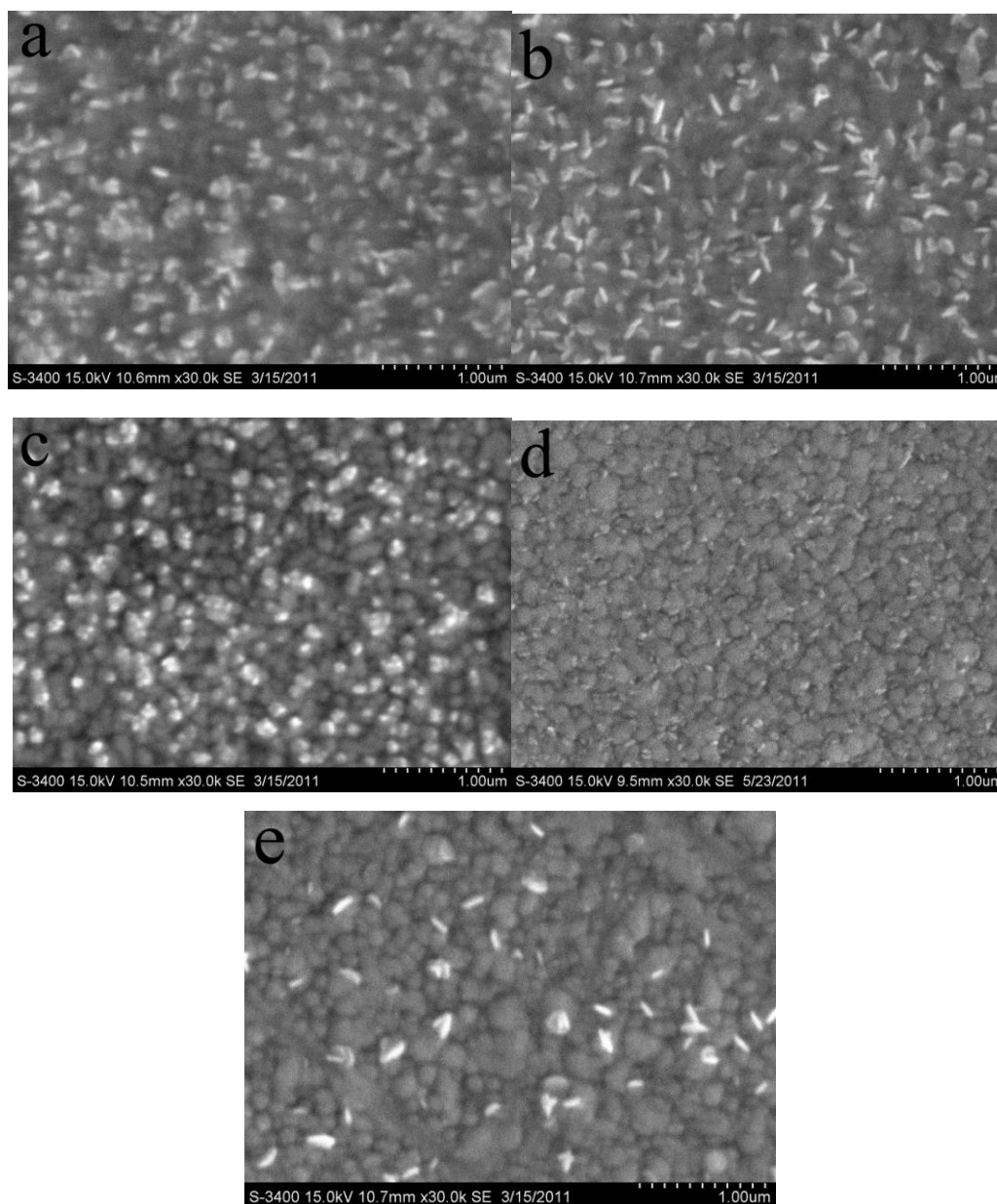


Fig. 2. SEM images of  $\text{CuInSe}_2$  films prepared at various sputtering temperatures: (a) 1h; (b) 2h; (c) 2.5h; (d) 3h; (e) 4h.

In addition, it can be seen in Fig. 2(d) that the texture morphology of CIS film prepared at 3.0 h CIS particles is well developed and an open porous columnar structure is obtained, the CdS particles are covered gradually which the grain size seems to be small. When the CIS film is prepared at 4.0 h (Fig. 2 (e)), CdS particles are covered completely and disappear on the surface.

It can be also seen from the Fig. 2 that the CIS particles diameter increases gradually as the increase of

sputtering times. When the sputtering time is less than 2.5 h, the morphology of the particles does not show a clear variation with the sputtering time. However, when the sputtering time reached to 3.0 and 4.0 h, the small particles are aggregated together and form the particles clusters which result in a relative rough surface. It can be observed that the particles with the big diameter are also composed of the small particles. As the sputtering time is increased to 3.0 and 4.0 h, these small particles get together again. However, the aggregations of these

particles are quite loose due to the low particles energy compared with that on short sputtering time (1, 2 and 2.5h).

### 3.3 Effects of sputtering time processes on optical properties

Fig. 3 shows the absorbance spectra as a function of wavelength for CuInSe<sub>2</sub> thin films of various times. It is easily noticeable that the absorbance in the visible region increased obviously with the increase of sputtering times. Obviously, the optical absorbance of the CIS film at 4.0 h is higher than the other films in the wavelength region above 300 nm. This is attributed to the increase in free-carrier absorbance due to the low electron mobility of the film [20]. Moreover, it also can be found that the change of absorbance is much faster in the 300-600nm region with the increase of sputtering times. Evidently, the long-time deposited processes not exceeding 4h cause a significant increase in the optical band gap close to the best absorbed band gap of sunlight. Therefore, controlling the optical band gap using the long-time deposited processes is a good way to enhance the conversion efficiency of a CIS solar cell.

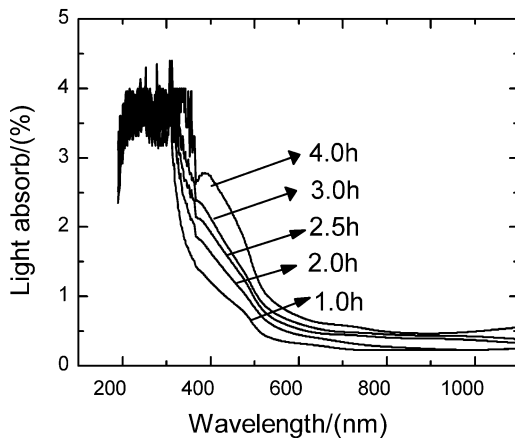


Fig.3. Absorption spectra of the CuInSe<sub>2</sub> films prepared at various sputtering times

It can be seen in Fig. 4 that the band gaps of the CIS films decreased with the increasing sputtering time. Evidently, the long-time sputtering processes (3.0 and 4.0h) can cause a significant increase in the optical band gap close to the best absorbed band gap of sunlight. In addition, it can also be observed that the short-time sputtering processes at 1.0, 2.0 and 2.5h can destroy the

CIS/CdS conductive layer with a high density of vacancy defects, which leads to a loss of positron trapping at these increased numbers of vacancies. Therefore, controlling the optical band gap using the long-time sputtering processes is a good way to enhance the conversion efficiency of a CIS solar cell.

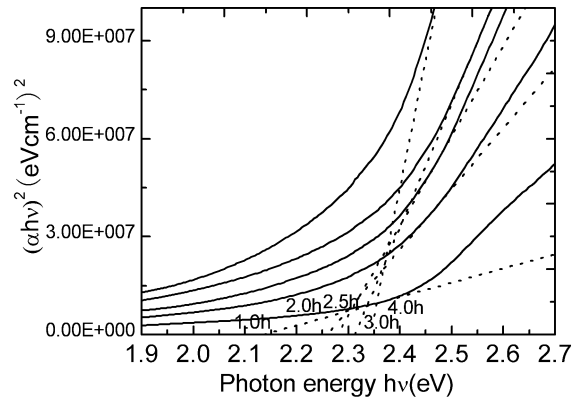


Fig.4. Plot of  $(\alpha h\nu)^2$  versus  $h\nu$  for the CuInSe<sub>2</sub> films prepared at various sputtering times

### 3.4 Effects of sputtering time processes on photoelectrical properties

Fig. 5 is I-V characteristic curves of the CIS thin-film batteries with different sputtering times. It can be seen in Fig. 5 that in the low temperature heating process (200 °C), the photoelectric conversion efficiencies of CIS film batteries increase from 1.14% to 5.56% and short circuit current density increase from 12.63 to 22.26 mA/cm<sup>2</sup> with the sputtering times increase from 1 to 4h. This suggests that the short circuit current density and the open circuit voltage of CIS thin-film batteries are very dependent on the film thickness. However, the thickness is too thick to the collection of the charge carrier, which is because the fill factor of the battery is so sensitive to the film thickness. In this result, it can be found in Fig. 5 that the sputtering time and film thickness is not enough to affect the fill factor of the battery.

In addition, there are a few factors that improving CIS thin-film batteries of the short circuit current density as well as the open circuit voltage as the increase of sputtering time of the battery. On the one hand, the short circuit current density depends on the circuit carrier collection in absorbing layer, which depends on the

thickness, optical absorbance of CIS absorbing layer and the draw ability of circuit carrier from the battery. On the other hand, the increase of battery thickness will reduce the electric field and make its redistribution, which will reduce the life of the free carrier and increase the space

charge. However, the open circuit voltage of battery depends on light carrier density and the band gap. Also, the introduction of defects will let the carrier of the interface area to produce composite phenomenon, which will limit the open circuit voltage.

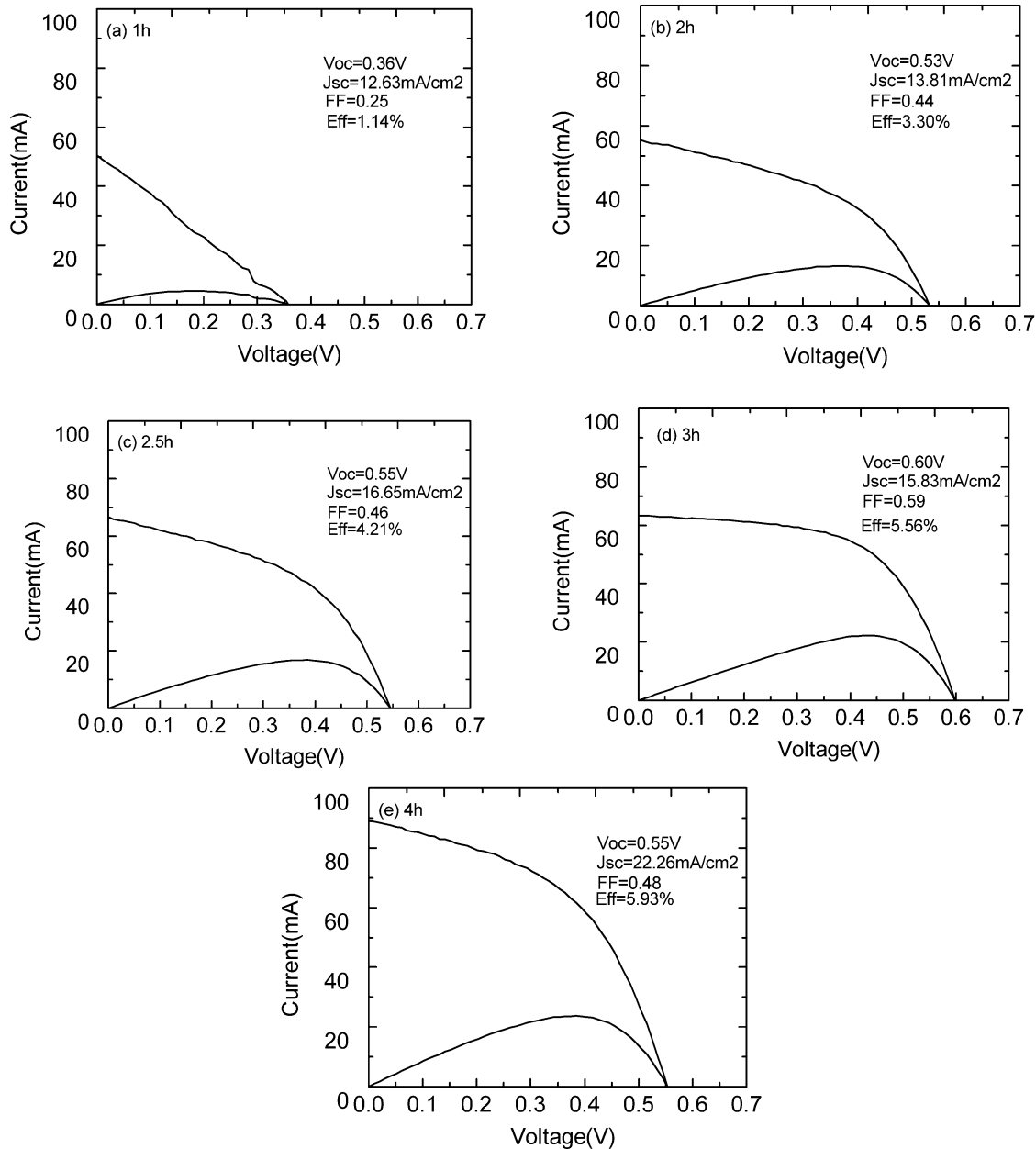


Fig.4. I-V characteristic curves of  $CuInSe_2$  films deposited at various sputtering times

#### 4. Conclusions

In conclusion, we systematically investigated the structural, optical and photoelectrical properties of  $CuInSe_2$  films with various sputtering time processes. The results show that long-time sputtering processes exceeding

to 3.0h can produce the particle aggregation and clusters to enhance the conversion efficiency of  $CuInSe_2$  solar cells. Long-time sputtering processes (2.5, 3.0 and 4.0h) are found to be vital for the transformation from the  $In_xSe$  phase to  $In_2Se_3$  and  $InSe$  structures. In addition, the optical absorbance result show that the optical absorbance of CIS

film at 4.0 h is higher than the other films in the wavelength region above 300 nm. Also, the long-time sputtering processes (3.0 and 4.0h) can cause a significant increase in the optical band gap close to the best absorbed band gap of sunlight. Finally, the I-V characteristic curves show that the photoelectric conversion efficiencies of CIS film batteries increase from 1.14% to 5.56% and short circuit current density increase from 12.63 to 22.26mA/cm<sup>2</sup> with the sputtering time increase from 1.0 to 4.0h. This suggests that the photoelectric conversion efficiencies and short circuit current density of CIS thin-film batteries are very dependent on the film thickness.

### Acknowledgements

This work is supported by the National Natural Science Foundation of China (Grant nos.11375112 and Grant nos.61176072).

### References

- [1] X. Ji, X. N. Wu, J. Y. Teng, Y. M. Mi, C. M. Zhang, L. J. Wang, *Optoelectron. Adv. Mater. - Rapid Comm.* **6**(11-12), 1081 (2012).
- [2] X. Ji, J. C. Deng, J. Y. Teng, Z. Yan, Y. M. Mi, C. M. Zhang, *Optoelectron. Adv. Mater. - Rapid Comm.* **7**(11-12), 845 (2013).
- [3] M. A. Popescu, *J. Non-Cryst. Solids.* **169**(1-2), 155 (1994).
- [4] M. A. Popescu, *J. Non-Cryst. Solids.* **35-36**, 549 (1980).
- [5] Haddou El Ghazi, A. Jorio, I. Zorkani, *J. Optoelectron. Adv. Mater.* **16**(11-12), 1242 (2014).
- [6] I. Banik, M. Popescu, *J. Optoelectron. Adv. Mater.* **16**(11-12), 1275 (2014).
- [7] R. S. Dariani, R. Zafari, *J. Optoelectron. Adv. Mater.* **16**(11-12), 1351 (2014).
- [8] P. M. Parameshwari, K. Gopalakrishna Naik, *J. Optoelectron. Adv. Mater.* **16**(11-12), 1361 (2014).
- [9] H. M. Mamedov, V. U. Mamedov, V. J. Mamedova, KH. M. Ahmadova, *J. Optoelectron. Adv. Mater.* **17**(1-2), 67 (2015).
- [10] B. Hymavathi, B. Rajesh Kumar, T. Subba Rao, *J. Optoelectron. Adv. Mater.* **17**(1-2), 160 (2015).
- [11] A. Azhagu Parvathi, K. Mathan Kumar, A. John Peter, *J. Optoelectron. Adv. Mater.* **17**(3-4), 343 (2015).
- [12] T. Munir, M. Umair, H.S. Munir, A. M Afzal, M. Rizwan, *J. Optoelectron. Adv. Mater.* **17**(3-4), 362 (2015).
- [13] U. Alver, S. Kerli, A. Tanriverdi, H. Yaykasli, *J. Optoelectron. Adv. Mater.* **17**(3-4), 439 (2015).
- [14] E. V. Krishnan, M. Al Ghabshi, Q. Zhou, K. R. Khan, M. F. Mahmood, Yanan Xu, Anjan Biswas, M. Belic, *J. Optoelectron. Adv. Mater.* **17**(3-4), 511 (2015).
- [15] A. Azhagu Parvathi, K. Mathan Kumar, A. John Peter, *J. Optoelectron. Adv. Mater.* **17**(5-6), 526 (2015).
- [16] E. Dinescu, C. Udrea, *J. Optoelectron. Adv. Mater.* **17**(5-6), 556 (2015).
- [17] Harit Kumar Sharma, P. K. Shukla, S. L. Agrawal, *J. Optoelectron. Adv. M.* **17**(5-6), 608 (2015).
- [18] S. Gagui, B. Hadjoudja, B. Chouial, B. Zaidi, Y. Kouhlane, N. Benslim, A. Chibani, *J. Optoelectron. Adv. Mater.* **17**(5-6), 670 (2015).
- [19] Yasin Khan, *J. Optoelectron. Adv. Mater.* **17**(5-6), 780 (2015).
- [20] S. Zhang, D. Sun, Y. Fu, H. Du, Q. Zhang, *Diamond Relat. Mater.* **13**, 1777 (2004).

\*Corresponding author: jixin@sues.edu.cn (Xin Ji)